PROPERTIES OF A CONTRACTED DISCHARGE IN A NONUNIFORM BOUNDARY LAYER ON AN ELECTRODE IN A HIGH-VELOCITY PLASMA FLOW

M. G. Musaev, É. K. Chekalin,
and L. V. Chernykh

UDC 537.533.5

The properties of an electric discharge in a high-velocity plasma flow in the presence of cold boundary layers on the electrode surface are of both scientific and practical interest. Unlike the diffusion regime of discharge current flow in boundary layers with a uniform distribution of the current density over the cathode surface [1], studies of the discharge-current regime in which cathode spots and microarcs form on the electrode surfaces in a high-velocity flow of electrically conducting gas are still far from complete [2].

In this paper we present the results of an experimental study of the structure of a discharge on electrodes and the corresponding current–voltage characteristics in pulsed supersonic plasma flows, as well as a semiempirical analysis of the data obtained.

In the experiments we employed a shock tube of the diaphragm type, consisting of two chambers [high pressure (HPC) and low pressure (LPC)], separated by a copper diaphragm 1 mm thick with a cross-shaped notch. The cylindrically shaped HPC, 100 mm in diameter and 1 m long, was filled with an oxygen–hydrogen fuel mixture (OHFM) with an addition of helium at a starting pressure of $4 \cdot 10^5$ Pa. The LPC consisted of a section with a circular steel tube 100 mm in diameter and 3.5 m long, a transitional section from the circular to a square cross section (72 × 72 mm) 200 mm long, a section of the channel with a square cross section (72 × 72 mm) 800 mm long, and a measuring dielectric section made of a Plexiglas block with a square cross section of the same size and 100 mm long with wall copper electrodes with a circular cross section 10 mm in diameter, flush-mounted on the surface of the channel and placed on opposite walls of the measurement section with special windows for optical observations of the processes occurring at the electrodes, The LPC was terminated with a section of channel with a square cross section and 900 mm long, attached to a receiver with a volume of 190 dm^3. The total length of the LPC thus equaled 5.5 m. An argon–hydrogen mixture with a hydrogen content of 10% at an initial pressure of $1.3 \cdot 10^3$ Pa was employed in the LPC.

Prior to filling the HPC and LPC with gas mixtures the chambers were evacuated to a pressure of 4 Pa and then flushed with the gas mixtures. The air mixture in the LPC constituted 0.1% of the working pressure of the gas mixture. After the explosion of the OHFM in the HPC, initiated with the help of a hot wire oriented along the axis of the HPC, the diaphragm opened up, gas expanded from the HPC into the LPC, and a strong shock wave (SW), compressing, heating, and accelerating the argon–hydrogen mixture up to a supersonic velocity, formed. The Mach number of the SW $M_1 \approx 12$, the equilibrium temperature of the plasma equaled 10^4 K, the velocity of the plasma behind the SW equaled 3500 m/sec, the Mach number of the flow $M_2 = 1.6$, and the pressure behind the SW equaled about $2 \cdot 10^5$ Pa. The transit time of the zone of shock-compressed gas (gas-dynamic plug) through the measuring chamber, placed in the region of steady-state SW velocity, equaled about 250 μsec. The velocity of the SW was measured with ionization monitors, arranged along the tube near the measuring section at fixed distances from one another. The pressure behind the SW was determined both computationally and experimentally with the help of a piezoelectric transducer. The equilibrium temperature and velocity of the flow of shock-compressed plasma were calculated from the conservation equations.

In studying the electrode processes the current oscillograms of the pulsed discharge of a capacitor bank with a total capacitance of $3 \cdot 10^{-3}$ F with a starting voltage of 150-550 V through an interelectrode gap with a shock-compressed plasma and serially connected load resistance ($R_L = 4\ \Omega$) were recorded. The high capacitance of the capacitor bank ensures that the source voltage remains virtually constant during the passage of the gas-dynamic plug; this makes it easier to analyze the current–voltage characteristics of the electrodes

Moscow. Translated from Zhurnal Prikladnoi Mekhaniki i Tekhnicheskoi Fiziki, No. 3, pp. 34-40, May-June, 1988. Original article submitted March 17, 1987.

 0021-8944/88/2903-0344$12.50

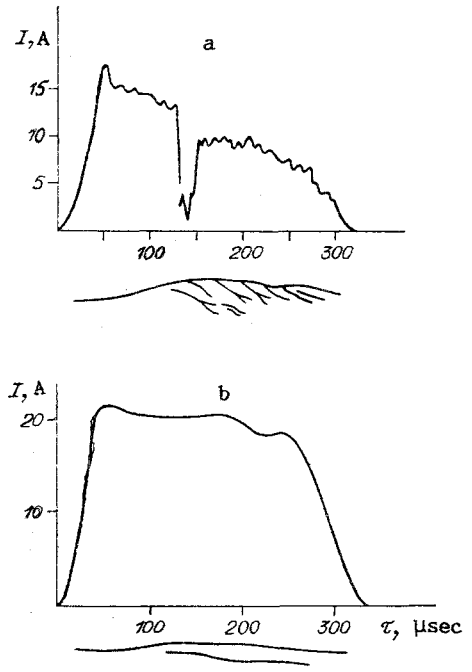

Fig. 1

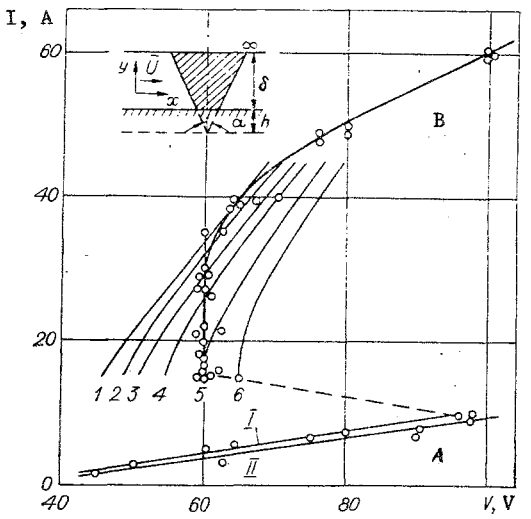

Fig. 2

based on the oscillograms of the discharge current. Photoscans of the discharge at the electrodes in the measuring section were recorded with the help of a high-speed drum-type camera, operating in the slave mode.

Figure 1 shows two current oscillograms of the discharge that are in phase with the corresponding photoscans of the discharge at the cathode for two different discharge current levels in the supersonic plasma flow with the parameters indicated above.

Figure 2 shows the experimental current–voltage characteristic, constructed based on the current oscillograms, referred to 75 μsec and consisting of two sections A and B, separated by a jump in the current and voltage.

Analysis of the photoscans and current–voltage characteristic shows that prior to the jump in the current and voltage (region A) the structure of the discharge luminescence at the electrode corresponds to nonstationary cathode spots (Fig. 1a), and up to 110 μsec one spot is observed. According to [2], the spreading of the current over the spot in the boundary layer occurs without Joule heating, contraction of the discharge, and formation of microarcs, penetrating the cold boundary layer and transforming into a diffusion discharge in an undisturbed plasma flow.

After the jump in the current and voltage on the current–voltage characteristics (region B) the traces of the cathode spots become wider and brighter (Fig. 1b); this is apparently caused by the formation of microarcs in the boundary layer [2].

Experiments performed with the help of a temperature sensor at the wall of the measuring section showed that the boundary layer remains laminar for approximately 110 μsec after the passage of the SW past the electrodes. The boundary layer then becomes turbulent, which, as follows from Fig. 1, leads to division of the cathode spots or formation of two microarcs burning simultaneously, depending on the current.

The current and voltage jump, owing to the formation of microarcs on an electrode, can apparently be explained by the overheating instability, when the current–voltage characteristics of the discharge and the microarcs satisfy the conditions for stable burning of an arc after the jump [3]. Further increase of the current causes the separated arcs to coalesce, a thin glowing section forms, and the glowing region of the plasma in the zone of contraction of the discharge on the electrode becomes wider.

Analysis of the region A of the current–voltage characteristic reduces to an examination of the spreading of the current from an isolated cathode spot in the laminar boundary layer with nonuniform electric conductivity across the layer. Let us assume that the current spreads from the spot within a sectioned cone, resting on the cathode spot, and also that there is no energy dissipation within the cone and the boundary layer is not heated by

the current. Let us assume further, following [2], that the current on the outer boundary of the boundary layer and in the core of the flow spreads out "hemispherically." The voltage drop in the boundary layer at the anode is determined experimentally. The voltage drop must be determined in all of the enumerated regions of the interelectrode gap and the data obtained must be compared with the total current–voltage characteristic A in Fig. 2.

In the theoretical analysis presented below it is assumed that the current-carrying sectioned cone with a half-aperture angle α_A rests on the cathode spot with radius r_0 and that, in addition, α_A and r_0 are independent of the current. The total voltage drop in the sectioned current-carrying cone without Joule heating will be determined in the form

$$V_{\delta_1} = \int_{\varepsilon}^{\delta} \frac{I_0 dy}{\pi\sigma (y+h)^2 \operatorname{tg}^2 \alpha_A}, \tag{1}$$

where the notation is the same as in Fig. 2, while I_0 is the current in the spot and $\sigma(y)$ is the electric conductivity in the laminar boundary layer. It is assumed here that the current is distributed uniformly in any transverse cross section of the sectioned cone.

Following [1], with the help of the computed dimensionless profiles of the electron density and temperature in the laminar boundary layer at the cathode, we determine in the ambipolar-diffusion approximation the profile of nonuniform electric conductivity in a laminar boundary layer, described by the relation

$$\sigma(y) = \sigma_\infty y/(1.2\delta) \tag{2}$$

(σ_∞ is the electric conductivity of the plasma at the outer boundary of the boundary layer).

The choice of the lower integration limit ε in (1) is difficult, since as $\varepsilon \to 0$ at the wall $\sigma_w \to 0$ and the integral diverges. For this reason, for definiteness, it was assumed that $\varepsilon = 10^{-3}$ cm, which corresponds to the geometric dimensions of the region of nonstationary cathodic spots [4]. The voltage drop at a copper cathode, according to [5], equals 11-12 V and is independent of the current in the spot.

Substituting the expression (2) into (1) and carrying out the integration, we obtain

$$V_{\delta_1} = \frac{1.2\delta I_0}{\pi\sigma_\infty r_0^2} \left[\ln \frac{\delta (\varepsilon \operatorname{tg}\alpha_A + r_0)}{\varepsilon (\delta \operatorname{tg}\alpha_A + r_0)} - \frac{(\delta - \varepsilon) r_0 \operatorname{tg}\alpha_A}{(\delta \operatorname{tg}\alpha_A + r_0)(\varepsilon \operatorname{tg}\alpha_A + r_0)} \right]. \tag{3}$$

The total voltage drop in the core of the flow, assuming "hemispherical" spreading of the current at the cathode and anode, was expressed in the form $V_\infty = \frac{I_0}{2\pi\sigma_\infty}\left(\frac{1}{R_c} + \frac{1}{R_a}\right)$ [R_c = $(\delta + h)\tan\alpha$ is the radius of the region of current flow on the outer boundary of the boundary layer at the cathode and R_a is the radius of the corresponding region at the anode and equal to the radius of the anode]. The total voltage drop in the interelectrode gap equals $V_\Sigma = V_{\delta_1} + V_\infty + V_c + V_a$ (V_c is the voltage drop at the cathode in cathodic spots and V_a is the anode voltage drop, including the boundary layer at the anode). With the help of electrostatic potential probes, placed on the insulating side walls of the measuring section in the shock tube, it was shown that in the region A of the current–voltage characteristic for $I \leq 10$ A $V_a = (2.2I_0 + 23)$V(I_0, A).

Among all indicated values of the voltage drop V_{δ_1} and V_∞ remain uncertain, since the value of α_A is unknown. The spreading half-angle of the current α_A is determined by comparison with the total experimental characteristic A in Fig. 2. The values of the constants in the relation (3) are presented below.

Satisfactory agreement between the experimental I and computed II data in Fig. 2 is obtained with $\varepsilon = 10^{-3}$ cm for $\alpha_A = 88°42'$, indicating that the current fills a significant volume of the laminar boundary layer.

Variation of ε from $2\cdot10^{-3}$ to $2\cdot10^{-4}$ cm, according to the relation (3), insignificantly changes the half-angle α_A (from 87°24' to 89°42'), apparently indicating that the voltage drop V_{δ_1} in the boundary layer remains stable when the thickness of the cathode layer changes in a random fashion. However, the above-proposed uniform current distribution over a large extent of the boundary layer is difficult to explain. The exact solution of the problem at hand has not yet been constructed.

To describe the properties and characteristics of microarcs in a laminar boundary layer in a high-velocity flow of conducting gas, we employed the equation of heat balance in the form

$$j^2/\sigma = C_p\rho U\nabla T - \mathrm{div}(\lambda\nabla T), \tag{4}$$

where the notation is standard.

The average plasma temperature T_g in a microarc was determined by integrating this equation with fixed boundary conditions, and the effective electric conductivity of the plasma and the corresponding voltage drop in a microarc were determined from it as a function of the current.

The following assumptions were made in integrating Eq. (4).

1. The processes in a microarc are studied in the two-dimensional approximation.
2. A microarc has the form of a sectioned cone, resting on a cathode spot of radius r_0 with half-angle α_B. The height of the arc equals the thickness of the laminar boundary layer (see Fig. 2).
3. The values of r_0 and α_B are independent of the current in the microarc, and are taken from experimental data.
4. Losses in the laminar boundary layer owing to heat conduction in the electrode and the surrounding gas are neglected; this is justified by estimates based on experimental conditions in a shock tube.
5. The value of ρU is everywhere constant in the boundary layer.
6. The distribution of the electric conductivity across the laminar boundary layer is described by the relation (2).
7. The current density in the transverse section of a microarc is constant.
8. The temperature and electric conductivity of the plasma are constant along the axis of a microarc.
9. The effective value of the electric conductivity in a microarc is defined as $\sigma_{eff} = \sigma_{max}/2$ (σ_{max} is the equilibrium electric conductivity of the plasma at the temperature T_g in a microarc).
10. The value of C_p averaged over the temperatures and transverse cross section of a microarc at its base is employed in the calculations; in addition, in the calculations C_p is assumed to be constant and independent of the temperature of the microarc.
11. In the microarc the temperature gradient along the flow $\nabla T_g = (T_g - kT_\infty)/r(y)$ (the coefficient k is obtained as a result of numerical integration taking into account the temperature distribution across a laminar boundary layer in the shock tube, presented in [1]).
12. The incident flow in the boundary layer partially penetrates into a microarc. The degree of penetrability $\xi = \rho_g U_g/(\rho_\infty U_\infty)$ depends on the current in the microarc, unlike other works (see, for example, [2]), where ξ was assumed to be constant.

Under the foregoing assumptions, integrating Eq. (4) in the two-dimensional approximation, we obtain an algebraic equation for T_g:

$$\underbrace{\frac{\sigma_\infty}{2}\left(\frac{T_g}{T_\infty}\right)^{3/4}\exp\left[8.7\left(1-\frac{T_\infty}{T_g}\right)\right]}_{\sigma_{eff}}\left[T_g - \frac{T_\infty}{\ln\left(\frac{\delta}{r_0}\operatorname{tg}\alpha_B + 1\right)}\right] = \frac{I_g^2\left[\frac{1}{r_0^3} - \frac{1}{(\delta\operatorname{tg}\alpha_B + r_0)}\right]}{3\pi^2 C_p \xi\rho_\infty U_\infty \ln\left(\frac{\delta}{r_0}\operatorname{tg}\alpha_B + 1\right)}. \tag{5}$$

The corresponding values of the effective equilibrium electric conductivity σ_{eff} were determined as a function of the arc current I_g and the parameter ξ with the help of Saha's formulas from the values of T_g found by solving Eq. (5) numerically; the sought voltage drops in the microarc are then determined from the conductivity as follows:

$$V_g = \frac{I_g\left[\frac{1}{h} - \frac{1}{(h+\delta)}\right]}{\pi\sigma_{eff}\operatorname{tg}^2\alpha_B} = \frac{3\delta C_p\xi\rho_\infty U_\infty\left[T_g\ln\left(\frac{\delta}{r_0}\operatorname{tg}\alpha_B + 1\right) - T_\infty\right]r_0^2}{I_g(r_0 + \delta\operatorname{tg}\alpha)}. \tag{6}$$

It follows from the right side of this relation that the voltage drop in a microarc increases as the thickness of the boundary layer δ increases and the plasma flux $\rho_\infty U_\infty$ increases, i.e.,

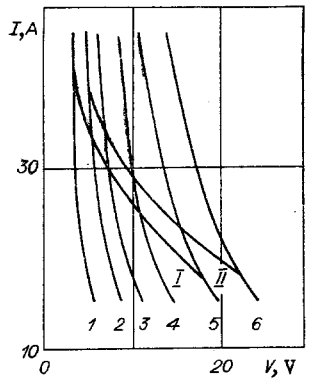

Fig. 3

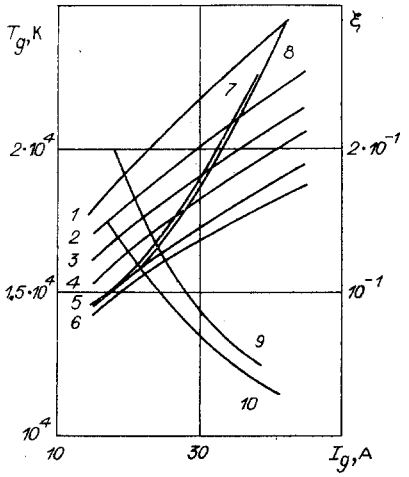

Fig. 4

the higher the convective losses in the microarc, the higher the voltage drop is.

The degree of penetrability of the flow into a microarc is not known a priori. Figure 3 shows the computed current–voltage characteristics of a microarc with ξ = const for a series of values of ξ [1) $\xi = 3\cdot10^{-2}$, 2) $5\cdot10^{-2}$, 3) $7\cdot10^{-2}$, 4) 10^{-1}, 5) $1.5\cdot10^{-1}$, 6) $2\cdot10^{-1}$] and C_p = 0.67 J/(g·deg). In calculating the characteristics the following values of the constant quantities were employed: δ = 0.175 cm, $U_\infty = 3.32\cdot10^5$ cm·sec^{-1}, $\rho_\infty = 10^{-4}$ g·cm^{-3}, $T_\infty = 10^4$ K, σ_∞ = 2.3 mho·cm^{-1} (all quantities are computed), $\tan\alpha_B$ = 0.33 (from the data of [6]), $r_0 = 2.2\cdot10^{-2}$ cm (based on traces of cathode spots on a polished electrode in one experiment), C_p = 0.67 J/(g·deg) is the value averaged in the range of temperatures T_g in Fig. 4 and over the transverse cross section of a microarc near its base, and C_p = 0.5 J/(g·deg) was employed to demonstrate the effect of the heat capacity on the computational results.

Figure 2 shows the family of total current–voltage characteristics $V_\Sigma(I_g)$ with ξ = const for the above-indicated values of ξ, obtained taking into account the data in Fig. 3. These characteristics were calculated using the data presented above for V_c and V_∞. The value of V_a, according to the probe measurements, in the region after the jump in the presence of anode spots and currents exceeding 15 A, was independent of the current and equaled approximately 16 V. The characteristics 1 to 5 cross the experimental total current–voltage characteristic. Assuming that the penetrability of a microarc varies along the experimental curve B in Fig. 2, and determining the values of ξ at the points of intersection as a function of the current, we construct the current–voltage characteristics of microarcs for C_p = 0.67 and 0.5 J/(g·deg) (lines I and II), presented in Fig. 3. It follows from here that the average value of C_p can substantially effect the computed value of the voltage drop in a microarc.

Figure 4 shows curves of the degree of penetrability versus the current I_g, obtained from the points of intersection in Fig. 2 for C_p = 0.5 and 0.67 J/(g·deg) (lines 9 and 10), as well as the current dependence of the plasma temperature in a microarc for variable ξ, corresponding to the experimental data, for C_p = 0.67 and 0.5 J/(g·deg) (lines 7 and 8), constructed with the help of the family T_g (I_g) with ξ = const. Figure 4 shows this family for ξ (same notation as in Fig. 3) with C_p = 0.67 J/(g·deg); one can see that the average value of C_p substantially affects the dependence $\xi(I_g)$ and has virtually no effect on T_g (I_g).

Thus as the current increases the temperature of the plasma in the arc increases and the penetrability parameter ξ decreases; in addition, $\xi \sim I_g^{-2}$, indicating that the magnetic pressure can affect the penetrability of the arc. In air-blown arcs, according to [7], two oppositely rotating, symmetric vortices form, so that the plasma in the vortices at the outer lateral boundary of the arc column moves in the same direction as the external flow. Then the plasma in the arc returns to the front surface of the arcs, thereby maintaining the stability of its electric conductivity. With this mechanism there is no need to replenish the mass of the arc with conducting gas – the plasma circulates in the arc, maintaining the required electrical conductivity. This is indicated by the low values of the degree of penetrability, close to the conditions of heat transfer with a solid body ($\xi = 3\cdot10^{-2}$), which was assumed in [2].

It should be noted that the conical structure of a microarc was the only structure satisfying the experimental current–voltage characteristics. Analogous calculations performed for other models, including cylindrical models with current flowing in both from the endface of the cylinder and through the side surfaces, gave voltage drops in the arc differing by several factors from the experimental data. Calculations for a cone with a lateral current gave results that are close to the model of a cone with an endface current.

Analysis of the effect of the uncertainty in the values of r_0 and $\tan\alpha_B$, which are given in calculations of T_g, σ_{eff}, and V_g, based on the relations (5) and (6), show that an error in the experimental determination of r_0 of ±10% leads to an error of ±4.5% in T_g, ±29% in σ_{eff}, and ±29% in V_g. At the same time a ±10% error in determining $\tan\alpha_B$ leads to an error of ±0.05% in T_g, ±0.3% in σ_{eff}, and ±0.3% in V_g.

Thus the voltage drop in a microarc is most sensitive to the size of the cathode spot. Therefore it must be assumed that the stability of the microarc will be guaranteed only if the dimensions of the cathode spots are stable.

To predict reliably the current–voltage characteristics of microarcs, the size of the cathode spot on which the microarc rests must be measured carefully and with high accuracy. The size of the spot determines the current density in the base of the microarc, which in its turn affects the liberation of heat, ionization, electric conductivity, and the current–voltage characteristic of the microarc.

At the present time there is no complete and correct theory of processes in arcs in a gas flow. The foregoing analysis shows that the degree of penetrability in arcs in a strong flow probably depends on the current; the higher the current and the temperature of the arc, the smaller is the penetration of the gas into the arc.

In conclusion, we call attention to the fact that the processes occurring under the conditions of highly nonuniform boundary layers in high-velocity flows are very complicated and they are coupled; this is why many serious assumptions and conjectures were made in the foregoing analysis of the experimental data.

LITERATURE CITED

1. É. K. Chekalin and L. V. Chernykh, "Experimental probe in low-temperature plasma flow," Zh. Prikl. Mekh. Tekh. Fiz., No. 1 (1981).
2. N. N. Baranov, M. S. Benilov, Z. G. Kamalov, and V. I. Kovbasyuk, "Experimental study of the characteristics of a contracted discharge on electrodes of an MHD generator," Preprint No. 3-178, Institute of High Temperatures of the USSR Academy of Sciences, Moscow (1985).
3. A. V. Nedospasov and V. D. Khait, Oscillations and Instability in Low-Temperature Plasma [in Russian], Nauka, Moscow (1979).
4. V. I. Rakhovskii, Physical Foundations of the Commutation of Electric Current in a Vacuum [in Russian], Nauka, Moscow (1970).
5. É. K. Chekalin and V. M. Gribkov, "Measurement of the near-electrode voltage drop in nonstationary cathode spots," in: Flow of Low-Temperature Plasma and Its Interaction with Channel Walls [in Russian], No. 26, G. M. Kpzhizhanovskii Energy Institute, Moscow (1974).
6. J. B. Heywood (ed.), Open-Cycle Magnetohydrodynamic Generators [Russian translation], Mir, Moscow (1972).
7. M. F. Zhukov, A. S. Koroteev, and B. A. Uryukov, Applied Dynamics of Thermal Plasma [in Russian], Nauka, Novosibirsk (1975).